

RESEARCH LETTER

Antibiotic Treatment Leads to Fecal *Escherichia coli* and Coliphage Expansion in Severely Malnourished Diarrhea Patients



Malnutrition predisposes to diarrhea and diarrhea adversely affects the nutritional status creating a vicious cycle.¹ The role of the gut microbiome in malnutrition is an active research area.² Parenteral antibiotics are recommended by the World Health Organization in hospitalized pediatric patients with severe acute malnutrition (SAM) presenting signs of infections.³ Stool microbiota data for such patients are, however, lacking. To fill this gap, we studied the stool microbiota in 19 SAM patients from Bangladesh hospitalized with acute diarrhea (AD) and compared it with that of matched 20 healthy control

subjects (HC) ([Supplementary Table 1](#)). SAM-AD patients were treated with parenterally administered gentamycin and ampicillin, whereas HC received no antibiotics for at least a month before sample collection.

16S rRNA and metagenome sequencing showed a marked increase of *Escherichia* and *Klebsiella* abundances in SAM-AD over HC ([Figures 1A, 1C, and 2A](#)), but not of *Streptococcus* ([Figure 1B](#)). Compared with HC, SAM-AD showed a reduced microbiota diversity ([Figure 1D](#)) and a decrease in *Prevotella*, *Blautia*, *Ruminococcus*, *Faecalibacterium*, *Megamonas*, and *Bifidobacterium* ([Figures 1A and 2A](#)). SAM-AD patients showed a 10-fold-lower 16S copy number of stool bacteria than HC ([Figure 1E](#)), which was partially compensated by a 2-fold higher stool frequency.

Rotavirus was the dominant pathogen ([Supplementary Table 2](#)) in SAM-AD, contradicting reports on protection from rotavirus diarrhea by malnutrition.⁴ All other pathogens (*Escherichia*

coli in 7, *Cryptosporidium* in 2, *Vibrio cholerae* in 1, norovirus in 1 patient), except in 1 patient with adenovirus, were associated with copathogens. *Salmonella* was not detected in any SAM-AD patient.

Compared with HC, virulence factor genes were increased in SAM-AD for various pathogenic Enterobacteriaceae (uropathogenic, enterohemorrhagic, and enteroaggregative *E coli*, *Shigella*, *Salmonella*, and *Yersinia*) ([Figure 2B](#)). The top 10 most significant pathway changes in SAM-AD over HC ([Supplementary Table 3](#)) included increases in D-glucarate and D-galactarate degradation genes ([Figure 2D](#)). In addition, SAM-AD showed more antibiotic resistance genes than HC ([Figure 2E](#)), mostly *E coli* (63%) and *Klebsiella* (32%) associated.

Escherichia phage followed by *Vibrio* phage DNA was increased in SAM-AD over HC ([Figures 2A and 2F](#)). The expansion of coliphages in SAM-AD was likely a consequence of increased abundance of bacterial host cells. Other mechanisms could play a role, such as

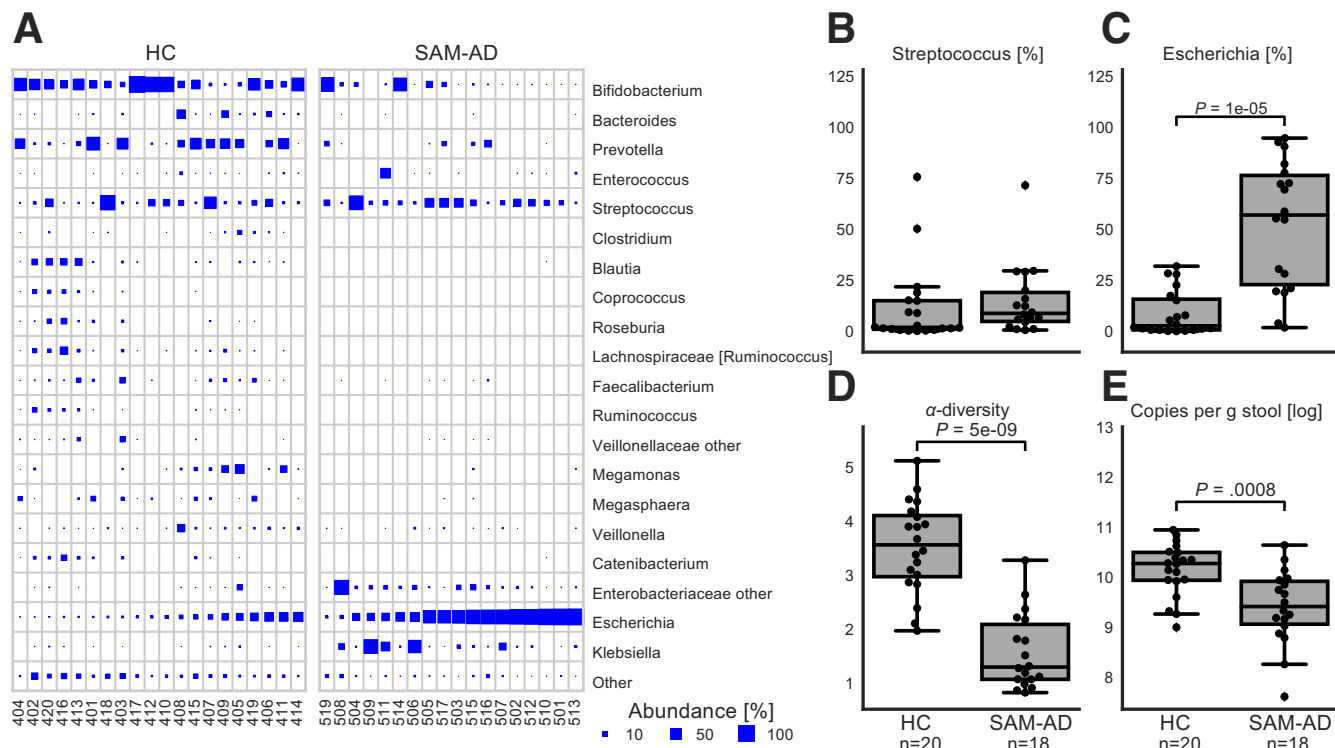


Figure 1. Stool microbiota analysis by 16S rRNA gene sequencing. (A) Bubble plot for 20 HC subjects and 18 SAM-AD cases at genus level. Box plots for *Streptococcus*- (B) and *Escherichia*- (C) attributed sequences, alpha-diversity (D), and log₁₀ copy numbers of 16S rRNA genes per gram stool (E).

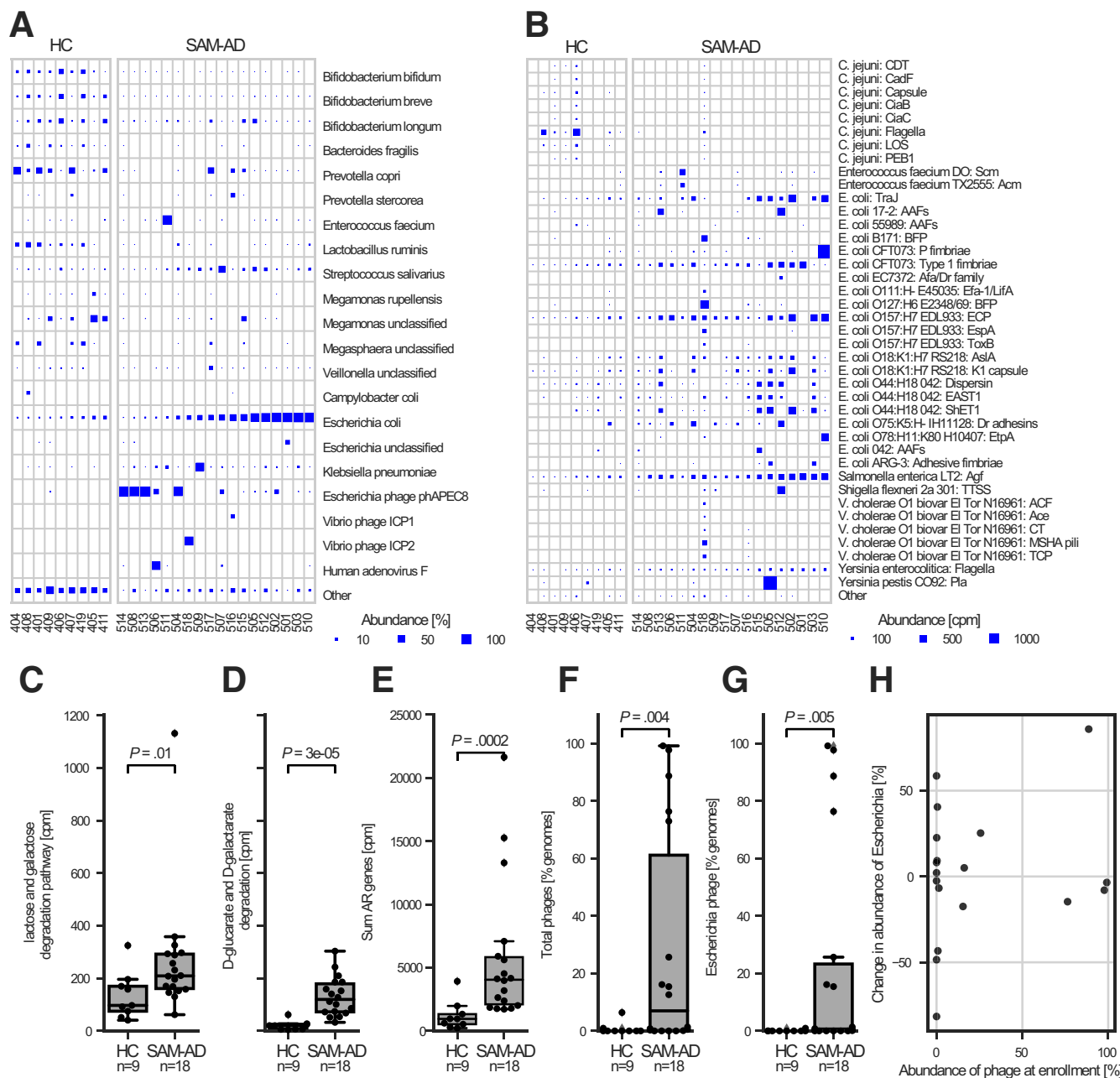


Figure 2. Stool microbiome analysis by metagenome sequencing. (A) Taxonomical attribution of sequences from 9 HC subjects and 18 SAM-AD cases to the indicated bacteria and viruses. (B) Attribution of the listed virulence factor genes to cases and control subjects given as counts per million genes. Abundance of sugar and sugar derivate-digesting genes (C, D) and antibiotic-resistance genes (E) in counts per million. (F) Abundance of indicated phage sequences expressed as percentage of total attributed sequences normalized for genome size by MetaPhiAn2. (G) Correlation between the abundance of the reads attributed to *Escherichia* phage phAPEC8 at hospitalization and change in abundance of *Escherichia* over a period of 1.5 days estimated by 16S rRNA sequencing.

increased accessibility or modified physiology of the bacterial host cells, for example as a consequence of immune system response to bacteria. Among SAM-AD patients, the abundance of sequences attributed to *Escherichia* phage phAPEC8 was negatively correlated with the abundance of

its host (Figure 2A, SparCC [1000 bootstraps]: -0.52; N = 18; P = .008). It is unclear, however, whether coliphage expansion could lead to a collapse of *E. coli* population because high abundance of phage at enrollment was not associated with a greater decrease of *E. coli* abundance over a

period of approximately 1 day (Figure 2G). Longer time series are necessary to determine whether bacteriophages could indeed control the expansion of host bacteria in the gut. Previous attempt to treat *E. coli*-associated AD with a mixture of T4 bacteriophages had failed to

demonstrate clinical benefit⁵; however, the *E coli* dominance was much more pronounced in antibiotic-treated SAM-AD patients of the present study than in children with AD.

A marked increase of fecal *E coli* abundance at the expense of bifidobacteria was also described in European newborns not suffering from diarrhea but treated parenterally with ampicillin and gentamicin for suspected sepsis.⁶ Postantibiotics expansion of *E coli* and *Salmonella typhimurium* was also observed in mice model⁷ where it was shown to be a consequence of streptomycin-induced production of galactarate and glucarate in host's cecum. This host-dependent mechanism may have contributed to the observed expansion of *E coli*, although the main driver was likely the high levels of antibiotic resistance displayed by *E coli* in Bangladesh.⁸ We think that the treatment with antibiotics rather than malnutrition and diarrhea was the main cause of the observed microbiota alteration, because Bangladeshi children with AD showed an increased abundance of commensal streptococci over control subjects,⁵ whereas children with SAM displayed a shift to a less mature fecal microbiota composition but not a marked *E coli* expansion.⁹

Antibiotic-induced Enterobacteriaceae expansion studied in mice has been shown to be involved in the disruption of the symbiosis between colonocytes and obligate anaerobic butyrate producers, resulting in a vicious cycle whereby colonocyte metabolism is subverted to permit the outgrowth of oxygen-tolerant, nitrate-dependent Enterobacteriaceae.¹⁰ It is known that antibiotic treatment in humans may lead to diarrhea even in a presumed absence of obligate pathogens (antibiotic-associated diarrhea), but the microbiota of pediatric antibiotic-associated diarrhea has not been studied.

Currently, there is no evidence from humans that the antibiotic-induced expansion of normally commensal Enterobacteriaceae could be detrimental. However, the observations from animal models suggest that this is a possibility that should be investigated.

SILAS KIESER,^{1,*} SHAFIQUL A. SARKER,^{2,*}
BERNARD BERGER,¹

SHAMIMA SULTANA,²

MOHAMMAD J. CHISTI,²

SHOEB B. ISLAM,²

FRANCIS FOATA,¹ NADINE PORTA,¹

BERTRAND BETRISEY,³

CORALIE FOURNIER,³

PATRICK DESCOMBES,³

ANNICK MERCENIER,¹

OLGA SAKWINSKA,¹

HARALD BRÜSSOW,^{1,†}

¹Nestlé Research Centre, Nutrition and

Health Research, Lausanne, Switzerland

²International Centre for Diarrheal

Diseases Research, Bangladesh, Dhaka,

Bangladesh

³Nestlé Institute of Health Sciences,

Lausanne, Switzerland

Corresponding author: Olga Sakwinska, PhD, PO Box 44, CH-1000 Lausanne 26, Switzerland. e-mail: olga.sakwinska@rdls.nestle.com; fax: + 41 21 785 8444.

Antimicrob Agents Chemother 2012;56:5811–5820.

7. Faber F, et al. Host-mediated sugar oxidation promotes post-antibiotic pathogen expansion. *Nature* 2016; 534:697–699.

8. Rahman MM, et al. Prevalence of extended spectrum-lactamase-producing *Escherichia coli* and *Klebsiella pneumoniae* in an urban hospital in Dhaka, Bangladesh. *Int J Antimicrob Agents* 2004;24:508–510.

9. Subramanian S, et al. Persistent gut microbiota immaturity in malnourished Bangladeshi children. *Nature* 2014;510:417–421.

10. Byndloss MX, et al. Microbiota-activated PPAR-g signaling inhibits dysbiotic Enterobacteriaceae expansion. *Science* 2017;357: 570–575.

*These authors contributed equally to the work.

†Current address: KU Leuven, Division of Animal and Human Health Engineering, Leuven, Belgium.

Most current article

© 2018 The Authors. Published by Elsevier Inc. on behalf of the AGA Institute. This is an open access article under the CC BY-NC-ND license (<http://creativecommons.org/licenses/by-nc-nd/4.0/>). 2352-345X
<https://doi.org/10.1016/j.jcmgh.2017.11.014>

References

- Guerrant RL, et al. Malnutrition as an enteric infectious disease with long-term effects on child development. *Nutr Rev* 2008;66: 487–505.
- Blanton LV, et al. Childhood undernutrition, the gut microbiota, and microbiota-directed therapeutics. *Science* 2016;352:aad9359.
- Lazzerini M, et al. Antibiotics in severely malnourished children: systematic review of efficacy, safety and pharmacokinetics. *Bull World Health Organ* 2011;89: 593–606.
- Verkerke H, et al. Malnutrition is associated with protection from rotavirus diarrhea: evidence from a longitudinal birth cohort study in Bangladesh. *J Clin Microbiol* 2016; 54:2568–2574.
- Sarker SA, et al. Oral phage therapy of acute bacterial diarrhea with two coliphage preparations: a randomized trial in children from Bangladesh. *EBioMedicine* 2016;4: 124–137.
- Fouhy F, et al. High-throughput sequencing reveals the incomplete, short-term recovery of infant gut microbiota following parenteral antibiotic treatment with ampicillin and gentamicin.

Author contributions

Silas Kieser: analysis and interpretation of data, and critical revision of the manuscript for important intellectual content statistical analysis. Shafiqul A. Sarker: study concept and design, patient recruitment, and critical revision of the manuscript for important intellectual content. Bernard Berger: analysis and interpretation of data, and critical revision of the manuscript for important intellectual content. Shamima Sultana: patient recruitment, and study supervision. Mohammed J. Chisti: patient recruitment. Shoeb B. Islam: patient recruitment. Francis Foata: acquisition and analysis of data, and technical support. Nadine Porta: acquisition of data, and technical support. Bertrand Betrisey: acquisition of data, and technical support. Coralie Fournier: acquisition of data, and technical support. Patrick Descombes: study supervision, and critical revision of the manuscript for important intellectual content. Annick Mercenier: critical revision of the manuscript for important intellectual content. Olga Sakwinska: analysis and interpretation of data, study supervision, and critical revision of the manuscript for important intellectual content. Harald Brüssow: study concept and design, study supervision, and drafting of the manuscript.

Conflicts of interest

The authors disclose no conflicts.

Funding

The study was funded by Nestec SA.

Supplementary Information

Patient Characteristics

The study was approved by the Ethical Review Committee of the International Center for Diarrhoeal Diseases Research in Dhaka, Bangladesh (icddr,b) as protocol #PR-14081. A total of 19 children with severe acute malnutrition (SAM) and acute diarrhea (AD) and 20 matched healthy control (HC) children were enrolled in Dhaka, Bangladesh during the winter season 2014–2015 (Supplementary Table 1). SAM-AD showed z scores <-3 indicative of severe underweight, severe stunting, and severe wasting. Because healthy children do not present to the icddr,b hospital, the control children were recruited at a field clinic maintained by icddr,b (Nandipara), whose population corresponds socioeconomically to the children hospitalized at icddr,b.

SAM-AD patients received reduced osmolarity oral rehydration solution supplemented with zinc for diarrhea treatment. SAM-AD is typically associated with a case-fatality rate of 30%–50% because of a high rate of manifest or developing infectious comorbidity (pneumonia, bacteremia, urinary tract infections). Therefore, as recommended by the World Health Organization,¹ all SAM-AD were treated on hospitalization with ampicillin (100 mg/kg/day in 4 doses for 48 hours by intravenous injection) and gentamicin (6 mg/kg/d in 2 doses by intramuscular injection) followed with amoxicillin (50 mg/kg/day in 3 divided doses given orally for 5 days). None of the control subjects had received antibiotics for a month before stool sampling.

No difference was seen for family income (HC, 7:8:5 and SAM, 6:9:4 with very low:low:moderate income; $P = .90$), maternal education (illiterate: HC, 2; SAM, 1; $P = .96$; primary school: HC, 12; SAM, 11; $P = .57$), or numbers of siblings (for 1, 2, 3, >3 children: HC, 10:4:5:1; SAM, 9:9:1:0; $P = .13$). Vaccination status was comparable in both groups (HC, 10 and SAM, 13 vaccination completed or running; $P = .4$) and feeding mode at 6 months of age (HC, 15:1:4; SAM, 10:4:5 exclusive breastfeeding vs formula feeding vs partial breastfeeding;

$P = .24$). However, the 2 groups differed for sex (HC, 12:8 and SAM, 3:16 for female:male; $P = .01$) (Supplementary Table 4) and previous exposure to cow's milk (HC, 7 and SAM, 18; $P = .003$).

Stool samples were obtained from the patients at enrollment into the study and the time of transfer to refeeding ward (1.6 + 1.4 days later). Samples were frozen at -80°C immediately after collection.

16S rRNA Sequencing

Total stool DNA was extracted using the QIAamp DNA Stool Mini Kit (QIAGEN, Hilden, Germany), following the manufacturer's instructions, except for addition of a series of mechanical disruption steps using a FastPrep apparatus and Lysing Matrix B tubes (MP Biochemicals, Santa Ana, CA).² 16S variable region V3 to V4 were polymerase chain reaction amplified using universal DNA primers with dual indexing³ and sequenced with MiSeq reagent kit V3 (Illumina Inc, San Diego, CA) as previously described.⁴ Raw sequence data were analyzed using Mothur V.1.33.0 21 and QIIME V.1.8 22 software packages.^{5,6} Paired-end sequences were demultiplexed and joined as described.⁵ Chimeras were identified and removed. Open reference OTUs picking at 97% identity used pick_ottus.py, with options usearch_ref.⁷ Taxonomy assignment used RDP Classifier⁸ on representative sequences. The resulting multiple alignments were used to build a phylogenetic tree with the FastTree method.⁹ Alpha-diversity was reported as the average of 10 rarefactions.

Metagenomics

Stool DNA was extracted using MoBio PowerMag Microbiome DNA Isolation Kit (QIAGEN, Hilden, Germany) on an epMotion M5073 (Vaudaux-Eppendorf AG, Basel, Switzerland) followed by Zymo DNA Clean & Concentrator Kit (Zymo Research, Irvine, CA). Library preparation was done according to the Nextera XT protocol from Illumina. The quality and quantity check was based on LabChip GX Touch HT (Perkin Elmer, Waltham, MA) results. Sequencing was performed on HiSeq

2500 using chemistry HighOutput v4 PE125 (Illumina). The paired-end reads were filtered using KneadData v0.5.1 (<https://bitbucket.org/biobakery/kneaddata>), which included quality filtering based on Trimmomatic and excluded reads mapping to the human genome. A median number of 3.2×10^7 reads and a minimum of 2.2×10^7 reads per sample were evaluated.

Taxonomic profiles were generated with MetaPhlAn2 2.5.0.¹⁰ Functional annotation was performed with HUMANn2 v0.7.1 and integrated into pathways from the MetaCyc database.^{11,12} The number of reads are first normalized by the length of the reference genome and then by million reads (counts per million). Functional annotation was used to calculate the abundance of antibiotic resistance genes from CARD database.¹³

ShortBRED¹⁴ was used to profile the metagenomics samples for virulence factors from the VFDB database.¹⁵ The mapped reads were first normalized by million reads and then by the length of reference sequence (RPKM).

The crucial step of bead-beating was included in both protocols of DNA extraction, ensuring an equal efficiency of DNA extraction from Firmicutes, Actinobacteria, and *Bacteroides*. We found a good correlation between MetaPhlAn and 16S rRNA analysis excluding major differences introduced by the 2 DNA extraction methods.

Pathogen Detection

Pathogens were identified by TaqMan Array Card (Thermo Fisher Scientific, Waltham, MA) detecting 19 enteropathogens,¹⁶ providing semi-quantitative cycle threshold values for each target. We normalized the values with respect to the total bacteria by quantitative polymerase chain reaction using universal primers.¹⁷ We considered pathogens as detected when the cycle threshold value was lower than in HC children. For the pathogens that were not detected in HC (*Salmonella*, *Vibrio cholera*, *Ascaris*, *Cryptosporidium*, and *Trichuris*) a threshold of 35 was imputed. This was complemented by screening of the metagenome sequences for pathogen taxa, defined as taxa targeted by

TaqMan Array Card, including pathotypes of *Escherichia coli* and associated virulence factors.

Data Availability

16S rDNA and metagenome reads are available under the Bio Project accession numbers SRP100410 and SRP100895.

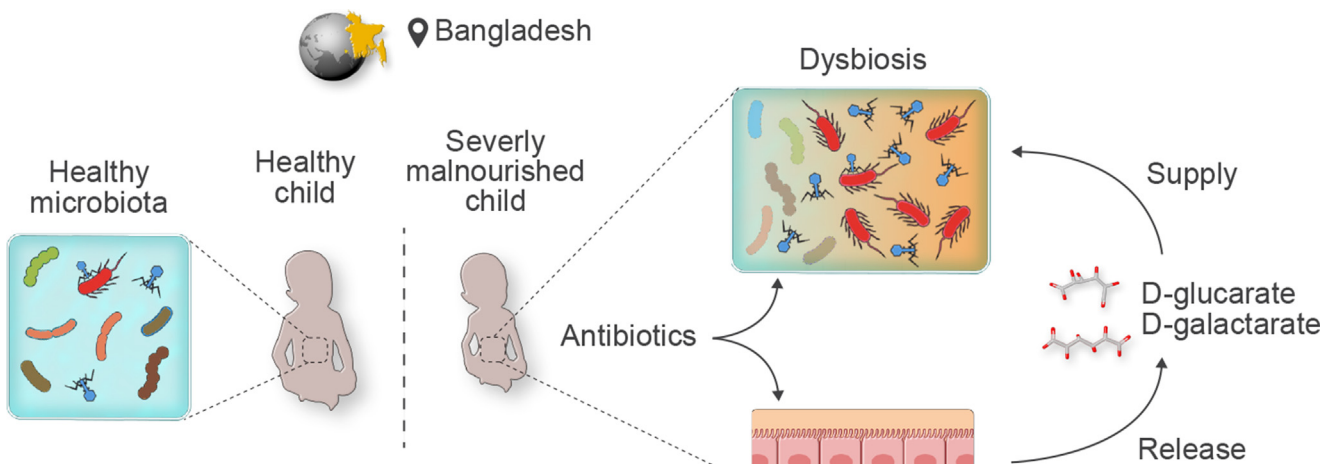
Statistics

Because microbiota abundance have a nonnormal distribution, nonparametric tests were used. The data met all assumptions of nonparametric tests. Nonparametrical tests do not require homoscedasticity for group comparison. If not otherwise mentioned the 2-sided Mann-Whitney test was used for continuous variables and a chi-square test for categorical variables. Data are shown as individual data points or as boxplots. In the boxplots the box represent the quintiles of the dataset, whereas the whisker extend to $1.5 \times$ the interquartile range.

Because the HC and SAM-AD differed in female/male ratio, we explored potential impact of sex on the major findings of the study. However, the children of the 2 sexes displayed similar findings (Supplementary Table 4).

References

1. Lazzarini M, et al. Antibiotics in severely malnourished children: systematic review of efficacy, safety and pharmacokinetics. Bull WHO 2011;89:594–607.
2. Junick J, Blaut M. Quantification of human fecal *Bifidobacterium* species by use of quantitative real-time PCR analysis targeting the *groEL* gene. Appl Environ Microbiol 2012;78:2613–2622.
3. Kozich JJ, et al. Development of a dual-index sequencing strategy and curation pipeline for analyzing amplicon sequence data on the MiSeq Illumina sequencing platform. Appl Environ Microbiol 2013; 79:5112–5120.
4. Caporaso JG, et al. Ultra-high-throughput microbial community analysis on the Illumina HiSeq and MiSeq platforms. ISME J 2012; 6:1621–1624.
5. Schloss PD, et al. Introducing mothur: open-source, platform-independent, community-supported software for describing and comparing microbial communities. Appl Environ Microbiol 2009; 75:7537–7541.
6. Caporaso JG, et al. QIIME allows analysis of high-throughput community sequencing data. Nat Methods 2010;7:335–336.
7. Edgar RC, et al. UCHIME improves sensitivity and speed of chimera detection. Bioinformatics 2011; 27:2194–2200.
8. Wang Q, et al. Naive Bayesian classifier for rapid assignment of rRNA sequences into the new bacterial taxonomy. Appl Environ Microbiol 2007;73:5261–5267.
9. Price MN, et al. FastTree: computing large minimum evolution trees with profiles instead of a distance matrix. Mol Biol Evol 2009;26:1641–1650.
10. Truong DT, et al. MetaPhlAn2 for enhanced metagenomic taxonomic profiling. Nat Methods 2015; 12:902–903.
11. Abubucker S, et al. Metabolic reconstruction for metagenomic data and its application to the human microbiome. PLoS Comput Biol 2012;8:e1002358.
12. Caspi R, et al. The MetaCyc database of metabolic pathways and enzymes and the BioCyc collection of pathway/genome databases. Nucleic Acids Res 2014; 42:D459–D471.
13. McArthur AG, et al. The comprehensive antibiotic resistance database. Antimicrob Agents Chemother 2013;57:3348–3357.
14. Kaminski J, et al. High-specificity targeted functional profiling in microbial communities with Short-BRED. PLoS Comput Biol 2015; 11:e1004557.
15. Chen L, et al. VFDB 2016: hierarchical and refined dataset for big data analysis—10 years on. Nucleic Acids Res 2016;44:D694–D697.
16. Platts-Mills JA, et al. Association between stool enteropathogen quantity and disease in Tanzanian children using TaqMan array cards: a nested case-control study. Am J Trop Med Hyg 2014;90:133–138.
17. Nadkarni MA, et al. Determination of bacterial load by real-time PCR using a broad-range (universal) probe and primers set. Microbiology 2002;148:257–266.



Supplemental Graphical Summary.

Supplementary Table 1. Baseline Characteristics of SAM-AD Case and Matched HC

	HC	SAM-AD	P value
N	20	19	
Age child, mo	13.0 (10.8 to 16.0)	13.0 (9.5 to 18.5)	.989
Age mother, y	25.5 (22.0 to 30.5)	24.0 (22.0 to 27.5)	.411
Weight, kg	8 (8 to 9)	5.9 (5.1 to 6.7)	2.93e-07
Height, cm	73.5 (69.8 to 77.4)	68.0 (64.5 to 70.7)	.0064
Mid arm circumference, cm	13 (13 to 14)	12 (11 to 12)	3.27e-05
Weight for age z score	-1 (-1 to -1)	-4 (-5 to -4)	1.01e-07
Height for age z score	-1 (-2 to -1)	-3 (-4 to -3)	4.35e-06
Body mass index	16 (15 to 16)	13 (12 to 13)	1.18e-07
Weight for height z score	-1 (-1 to -0)	-3 (-4 to -3)	1.01e-07
Body mass index z score	-0 (-1 to 0)	-3.4 (-4.2 to -2.8)	1.37e-07
Mid arm circumference z score	-1 (-1 to -1)	-3 (-3 to -3)	2.34e-05
Rectal temperature, °C	36.5 (36.0 to 36.7)	37.2 (37.0 to 37.2)	1.08e-07
Pulse, min ⁻¹	110.0 (100.0 to 120.0)	132.0 (130.0 to 136.0)	7.23e-08
Respiration rate, min ⁻¹	30.0 (30.0 to 32.0)	36.0 (35.0 to 36.0)	4.46e-07
Vomiting, d ⁻¹	0.0 (0.0 to 0.0)	0.0 (0.0 to 2.0)	.00345
Duration of diarrhea, d		4 (4 to 4)	
Stool frequency, d ⁻¹	2.5 (2.5 to 2.5)	5.0 (3.5 to 7.0)	6.15e-06
Systolic blood pressure, mm Hg	90.0 (90.0 to 90.0)	90.0 (90.0 to 90.0)	.0166
Diastolic blood pressure, mm Hg	60.0 (60.0 to 60.0)	60.0 (60.0 to 60.0)	.101
Exclusive breastfeeding, mo	6.0 (5.8 to 6.0)	6.0 (2.5 to 6.0)	.0578
Number of siblings	1.5 (1.0 to 3.0)	2.0 (1.0 to 2.0)	.541

NOTE. Values are medians (interquartile range: first, third quartile). P values are calculated by a 2-sided Mann-Whitney test. Categorical variables were compared by chi-square test.

Supplementary Table 2. Pathogen Detection in Stools of SAM-AD Patients

Patient ID	TaqMan	Pathogen taxa	<i>Escherichia coli</i> pathogens	Virulence factors
506	Adenovirus (8)	Adenovirus (67)	neg	neg
511	<i>Cryptosporidium</i> (3)	neg	neg	neg
503	Ascaris (3) Rotavirus (3)	neg	EAEC-aaiC (0.01)	EAEC-aaiC (154)
516	neg	<i>Shigella</i> (1)	neg	neg
518	<i>Vibrio cholerae</i> (7) EPEC-bfp (5) EPEC-eae (4) EIEC-ipaH (3)	<i>V cholerae</i> (3)	neg	EPEC -bfp (36)
517	<i>Cryptosporidium</i> (15) EPEC -bfp (6) EPEC-eae (6) EIEC-ipaH (6) EAEC-aaiC (5)	neg	neg	neg
513	NA	neg	EAEC-aaiC (0.01) EAEC-aatA (0.01)	EAEC-aaiC (120) EAEC-aatA (79)
515	Norovirus (5)	neg	EAEC-aaiC (0.01)	EAEC-aaiC (123) EAEC-aatA (78)
501	Rotavirus (10)	neg	neg	neg
502	Rotavirus (5) EAEC-aaiC (3)	neg	EAEC-aaiC (0.02)	EAEC-aaiC (275)
504	Rotavirus (12)	neg	neg	neg
505	Rotavirus (8) EAEC-aatA (3)	neg	EAEC-aaiC (0.01) EAEC-aatA (0.02)	EAEC-aaiC (202) EAEC-aatA (62)
507	Rotavirus (8)	Adenovirus (3) <i>Aeromonas</i> (0.2)	neg	neg
508	Rotavirus (6)	neg	neg	neg
510	Rotavirus (6)	neg	ETEC-It (0.03)	ETEC-It (346)
514	Rotavirus (11)	Adenovirus (0.1)	neg	neg
519	Rotavirus (10)	NA	NA	NA
509	neg	<i>Shigella</i> (0.5)	neg	neg
512	<i>Cryptosporidium</i> (9) EIEC-ipaH (3)	<i>Shigella</i> (2) <i>Cryptosporidium</i> (0.5)	neg	EAEC-aatA (114) EIEC-ipaH (36)

NOTE. TaqMan, results of detection of 19 pathogens with TaqMan array card (difference to threshold expressed as cycle threshold), *E coli* pathotypes and the detected virulence factors are indicated, neg, no pathogen detection; pathogen taxa, percentage of taxons determined in metagenome sequencing of the indicated pathogen, neg, <0.1% of taxa; *E coli* pathogens, the indicated virulence genes of the specified *E coli* pathotype with % of identified *E coli* genes, neg, <0.01 of genes; virulence factors, gene read number corrected per million reads and length of target gene coverage. NA, the corresponding sample was not investigated by metagenome sequencing.

Supplementary Table 3. Top 10 Pathways Significantly Enriched in SAM-AD Over HC in Stool Metagenome Data

Description	HC	SAM-AD	Q
Superpathway of L-arginine and L-ornithine degradation	13	105	0.0002
Superpathway of L-arginine, putrescine, and 4-aminobutanoate degradation	13	105	0.0002
D-glucarate degradation I	21	161	0.0004
Phytol degradation	45	391	0.0004
D-galactarate degradation I	20	120	0.0007
Superpathway of D-glucarate and D-galactarate degradation	20	120	0.0007
Methylphosphonate degradation I	11	94	0.0007
Superpathway of fermentation	48	179	0.0012
Phytate degradation I	28	218	0.0012
NAD/NADP-NADH/NADPH mitochondrial interconversion	32	177	0.0012

NOTE. Median counts per million reads as assessed by 1-sided Mann-Whitney *U* test corrected for multiple testing by the Benjamini-Hochberg procedure.

NAD, nicotinamide adenine dinucleotide; NADH, reduced nicotinamide adenine dinucleotide; NADP, nicotinamide adenine dinucleotide phosphate; NADPH, reduced nicotinamide adenine dinucleotide phosphate.

Supplementary Table 4. The Main Variables That Were Evaluated in the Study, Stratified By Sex

	HC		SAM-AD	
	Female	Male	Female	Male
16S rRNA sequencing				
N	12	8	2	16
<i>Bifidobacterium</i> (proportion of reads)	25.0 (6.62–47.1)	24.9 (18.8–55.6)	0.024 (0.02–0.02)	0.405 (0.05–6.07)
<i>Escherichia</i> (proportion of reads)	1.46 (0.71–9.76)	6.32 (1.95–24.1)	62.6 (46.6–78.6)	57.0 (20.8–73.8)
Diversity (Faith index)	4.007 (2.86–4.37)	3.308 (3.08–3.51)	1.360 (1.28–1.44)	1.306 (1.06–2.19)
Shotgun metagenomics				
N	12	8	3	16
Antibiotic resistance genes (counts per million reads)	955 (767–1213)	608 (530–1326)	4117 (3063–4140)	3978 (2115–6495)
D-galactarate degradation pathway (counts per million reads)	13.6 (6.94–30.50)	20.3 (5.65–25.30)	85.7 (78.80–119.01)	127 (70.90–186)
Phage sequences (percentage of total sequences, normalized for genome size)	0.469 (0.00–2.30)	0.000 (0.00–0.00)	73.0 (49.3–85.4)	0.794 (0.04–15.8)

NOTE. Median and interquartile range are displayed.